Journal of the Korean Nuclear Society
Volume 33, Number 5, pp.498~509, October, 2001

Study on the Improvement of Indirect Intra-Oral Dental Digital X-ray Image Sensor with Optical Coupling

Joo Ho Whang, Jin Bum Chung, and Tae Woo Kim
Kyunghee University
1 Seocheon-ri Kihung-eup, Yongin-shi, Kyungki-do, 449-701, Korea
jooho@khu.ac.kr

(Received May 24, 2001)

Abstract

Optimum characteristics of digital X-ray sensor components were analyzed to develop intra-oral dental digital X-ray image sensor using indirect method. Parametric analysis was carried out to optimize the phosphor thickness and the fiber optic plate (FOP) coupling to charge coupled device (CCD). X-ray absorption and light diffusion in the phosphor layer were analyzed by the Monte Carlo method. Real time X-ray image was obtained with prototype X-ray image sensor using general CCD camera with 1~10 lp/mm resolution. It has been previously shown that large resolution degradation in X-ray images was caused by miss alignment of FOP to CCD and optical adhesive selection. In this study, we reported that X-ray image quality was greatly improved by using optimized characteristics of alignment device and phosphor thickness.

Key Words : digital X-ray image sensor, X-ray, fiber optic plate(FOP), phosphor, charge coupled device(CCD)

1. Introduction

Digital X-ray system can be separated into direct and indirect method(Fig. 1). In direct method, X-ray emission by an object directly appear into an image that is further converted to electrical signal by digital image device[1]. Direct method can give high speed image because of its direct transmission to image device but needs exposure to higher dose than indirect method in human body. In the indirect method, X-ray emission by an object is first converted into light photons in the presence of phosphor. The resulting image is next converted to electrical signal by digital image device.

In this paper, we performed characteristic upgrade study of intra-oral dental digital X-ray image sensor using visible rays CCD from principle of digital X-ray image sensor by studying: 1) union characteristic composing X-ray image sensor combined with phosphor, FOP and CCD that are often used for intra oral dental digital X-ray image sensor and 2) optimum study of phosphor thickness which affects the resolution

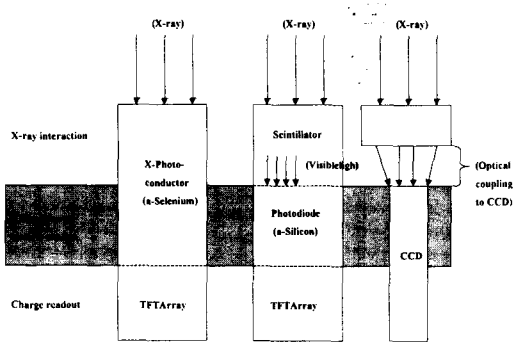

Fig.1. Detection Method of Digital System.

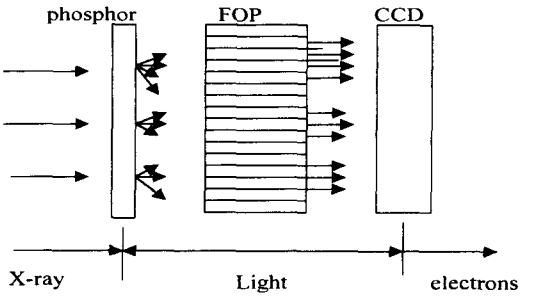

Fig. 2. Diagram of Dental Digital X-ray Image Sensor with Indirect Method

image gain and X-ray efficiency. Decision of optimum thickness was determined by three following methods: 1) X-ray absorption rate and distribution of phosphor, 2) light transport in phosphor and 3) derivation of optimum thickness. Several authors have investigated X-ray energy absorption of phosphor (Hamaker 1947, Ludwig 1971, and Swank 1973). Theoretic calculations assumed that photoelectric absorption is the only significant interaction. But we would calculate absorption energy concerned transmission and scattering using MCNP code. Also Swank 1973, Giger et al 1983 and Nishikawa et al 1990 introduced research of light diffusion in phosphor. Light transport function is described into theoretic calculate by them. However, we will depict it as energy absorbed in phosphor using DETECT97 code.

2. Component of Intra-oral Dental Digital X-ray Sensor

In digital system of a branch of intra oral radiation, various digital X-ray sensors are developed after introduction of Radio-Visio-Graphy using image element CCD in 1989, and digora from Soradex company using PSP(Phosphor Storage Plate). Besides, most of intra oral dental digital X-ray sensor that come into the market by now used CCD[2][8]. Almost intra oral dental digital X-ray sensor has a structure of phosphor: CCD that gets radiation image using phosphor, and indirect method with FOP transferable light signal optically between them (Fig. 2).

3. Optimization of Phosphor

3.1. Phosphor

3.1.1. Diffusion of Light in Phosphor

X-ray image using phosphor has a large difference in the quality as a characteristic of phosphor. Important parameters that affected resolution of phosphor are type of phosphor, size of phosphor particle, thickness homogeneity of phosphor layer and phosphor thickness. Incident X-ray reacting with phosphor is released all direction which is absorbed in the responding spot, and increased diffusion as the thickness. Therefore as the thickness, the diffusion of light photon in phosphor is shown by PSF(Point Spread Function) below. [7]

$$P(Z) = \int_{-Y}^{Y}\int_{-X}^{X} \frac{N_{opt}}{4\pi} \times \frac{z}{(x^2+y^2+z^2)^{2/3}}\, dxdy \quad (1)$$

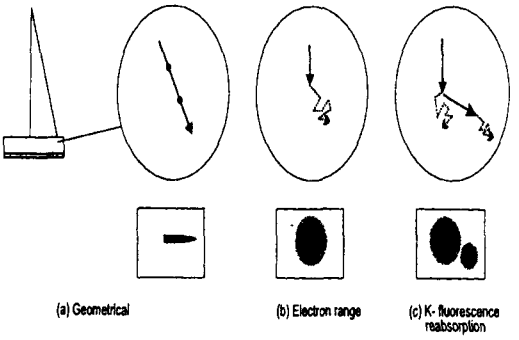

Fig. 3 Intrinsic Diffusion of Phosphor

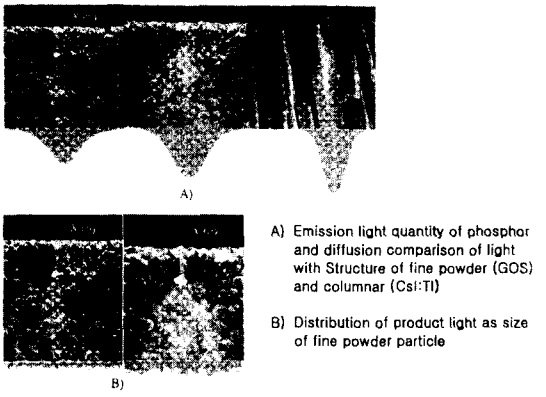

Fig. 4. Light Diffusion and Emission of Gd_2O_2S:Tb and CsI:Tl

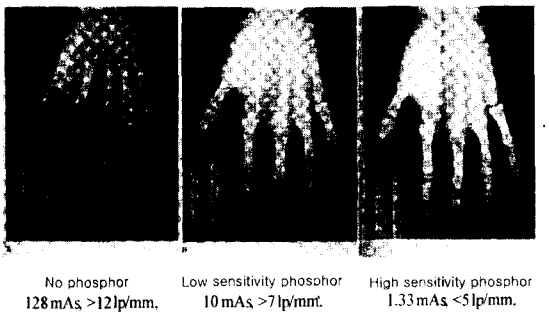

Fig. 5. Resolution Loss as Using of Gd_2O_2S:Tb

Where, P(z) is PSF, N_{opt} is light photon quantity produced in axis of x, y, z. X, Y are sampling pitch and x,y,z are position of the X-ray source. As shown Fig.3, the occurrence of characteristic X-ray by incident energy which over K-edge of phosphor or by surrounding absorption that caused electronic range like a spot of photon, Auger electron caused low resolution by effect of reabsorption in surrounding.

Most representative diagnosis radiation phosphor is Gd_2O_2S:Tb, fine powder and CsI:Tl, Columnar structure are rare on earth. These have a similar X-ray absorption rate and transform efficiency. Like FOP, CsI:Tl has a small diffusion in spite of increased thickness, but it is difficult to find and to exact growth of edge columnar structure. Besides it required special security equipment to avoid vapor. So in this study, we performed study for X-ray image sensor that applied Gd_2O_2S:Tb. Chat. 1 indicate that physical characteristic of main phosphor where, Γ represents releasing number of light photon per X-ray absorb quantity required to produce a light photon. These values are calculated in 100 % assuming that optic diode

Table 1. Phyysic Characteristic of Phoshor Using Diagnosis X-ray

Type	Z	K-edge (keV)	r(g/cm^3)	λ(nm)	Index of	W(eV)	G(light/keV)
CaWO4	74	69.5	6.06	480±100	2.25	33	30
Gd202S:Tb	64	50.2	7.34	550±20	2.3	17	60
CsI:Na	55/35	36/33	4.51	415±50	1.84	25	40
CsI:T1	55/35	36/33	4.51	560±80	1.79	18	55

NA of CCD. spectral sensitivity of CCD, separation probability of light photon in the phosphor. Therefore as these values changed Γ, W values also changed.

Fig. 4 indicates that light diffusion and release characteristic of Gd_2O_2S:Tb and CsI:Tl, also show that when light diffusion is high and has large fine power, it has a large light photon and vigorous diffusion activity[3]. Fig. 5 indicate a hand shape of the resolution fall according to phosphor using film*screen system. where, thick fluorescence screen indicates high sensitivity, thin fluorescence screen indicates low sensitivity, when there is no phosphor it has the best resolution and a lot of exposure dose.

3.1.2. Energy Absorption Efficiency

Incident X-ray in phosphor has a difference in the respondence spot that Quantum Detection Efficiency(QDE) and Energy Absorption Efficiency(EAE) by movement of characteristic X-ray and electron. X-ray detection substance was demanded response with X-ray incident to save information signal of X-ray in other word, X-ray information do not react with detection substance are lost. The design purpose of X-ray detector in medical radiation image is to maximum X-ray absorption efficiency relation to other performance variable which is given like space resolution. QDE shown below.

$$QDE = \frac{\int_{E=0}^{E_{max}} \Phi(E)(1 - e^{-\mu(E)x})dE}{\int_{E=0}^{E_{max}} \Phi(E)dE} \quad (2)$$

where, x is thickness of detection substance. μ(E) is linear attenuation coefficient. Φ(E) is X-ray spectrum (fluence per energy) However QDE is simple rate of incident X-ray photon which attenuated by detection substance. In direct of indirect X-ray detector image signal has relation to

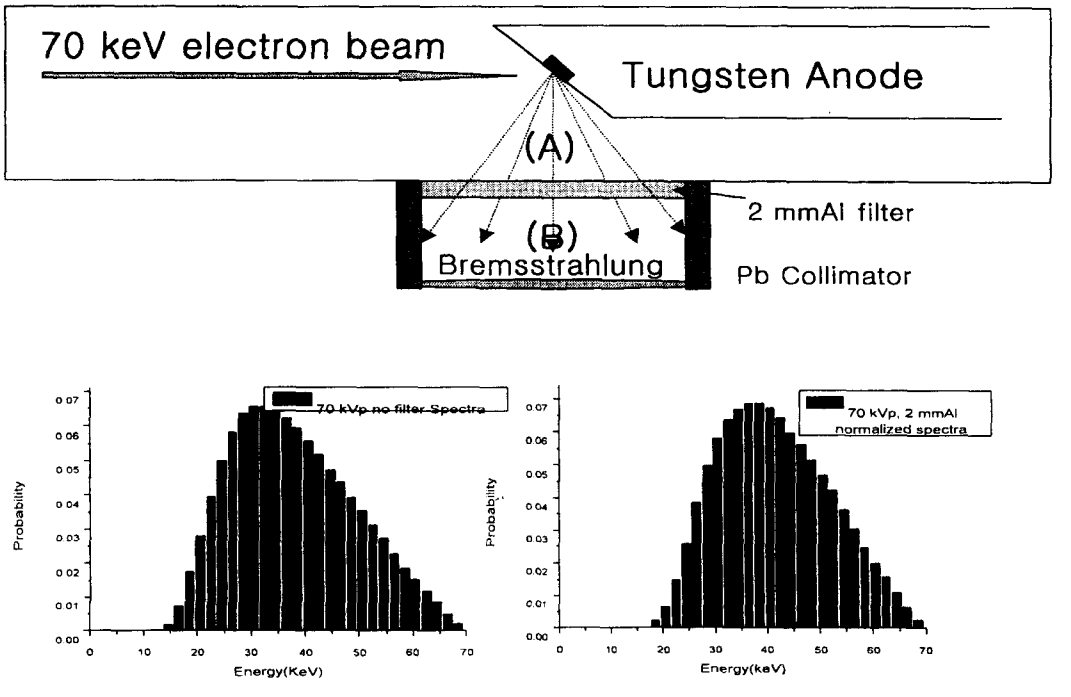

Fig. 6. X-ray Spectrum of 70 kVp Energy in Tungsten Target

not X-ray photon number but general energy absorption. EAE of detector shown below.

$$EAE=\frac{\int_{E=0}^{E_{max}}\Phi(E)E(\frac{\mu_{en}(E)}{\mu(E)})(1-e^{-\mu(E)x})dE}{\int_{E=0}^{E_{max}}\Phi(E)EdE} \quad (3)$$

The denominator of above expression indicates simple rate of energy that incident in X-ray detector per unit area. Also, $(1-e^{-mu(E)x})$ in numerator indicates the rate of X-ray photon incident from detector, absorption energy per incident X-ray photon defined by $E(\mu_{en}(E)/\mu(E))$ in the numerator. Therefore QDE and EAE have a difference because the energy that relation to characteristic X-ray is released again from detection substance if the energy over K-edge is entered. But this simulation was not considered characteristic X-ray effect because K-edge simulates energy absorption for Gd_2O_2S:Tb, 50.22 keV.

3.2. Monte-Carlo Code Phosphor Simulation

3.2.1. X-ray Spectrum

In general, X-ray intensity used by intra-oral dental clinic has tube voltage of 60~70 kVp and tube current of 8~10 mA. The thickness of Al filter is used in order to reduce exposure eliminating low X-ray energy.[1][6] In this paper, X-ray energy in the two poles of 70 kVp, 2 mmAl tungsten performed simulation using continuous spectrum of it' s average energy, 40 keV. After this, it is required a comparison with simulation using continuous energy X-ray spectrum for 70 kVp no filter of continuous energy takes a value from the "Handbook of Medical Imaging" and using MCNP code, simulated it which is passed 2 mmAl filter. Fig. 6 shows spectrum of 70 kVp. where, after passed 2 mmAl. we can see spectrum hardening. it has 40 keV average energy after passed 2 mmAl.

3.2.2. Simulation Method

Generally used tube voltage of dental X-ray is 60 ~70 kVp. In this simulation, X-ray tube voltage is 70 kVp, the distance between phosphor and focus is 20.5 cm, the size of phosphor is 5000 × 4000 μm, and simulated absorption and X-ray absorption distribution following every 10 μm pitch by 10~120 μm thickness. X-ray spectrum of real tube voltage, 70 kVp is continuous spectrum like Fig. 8. but in this simulation, we simulate for 40 keV mono energy, average energy.

This simulation calculated X-ray absorption distribution in MCNP code increasing Gd_2O_2S:Tb thickness and geometrical shape of phosphor calculated absorbed X-ray energy in each unit cell dividing 5000 × 4000 × 3 μm size unit cell to calculate X-ray absorption distribution like in hexagon on Fig. 7 below. Besides the source of X-ray was assumed that it is entered vertically in the middle of unit cell be in center of phosphor. In order to reduce statistical error, we setting 4,000,000 history of MCNP code. Besides we calculated light diffusion in absorption spot

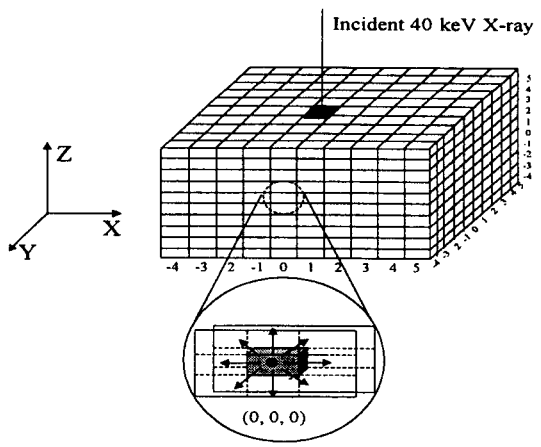

Fig. 7. Simulation Geometry of Phosphor

applicable at input of DETECT97 code, Monte-calro code simulating light transportation. we assumed that X-ray energy absorbed in unit cell is released in 4π direction creating a light in center of the cell. In simulation, we ignored that thought it is created a little light in the surrounding by fluorescence X-ray and rand of dispersion electron. Although real phosphor Gd_2O_2S:Tb is fine power, geometry of phosphor in this simulation represented by homogeneous substance but it is possible to simulate dispersion and absorb a light in the fine power applicable absorption distance(AD) 400 μm, scattering distance(SD) 25 μm of light in the inner phosphor.

3.2.3. Simulation Benchmark

To prove X-ray absorption and diffusion calculated by MCNP and DETECT97 code compared reference value. X-ray absorption used MCNP is equal to "Handbook of Medical Imaging", and MTF used DETECT97 is nearly equal to Fig. 8 which show MTF of Gd_2O_2S:Tb

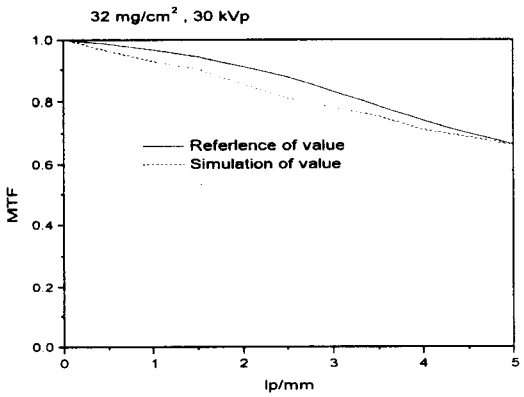

Fig. 8. MTF Benchmarking

32 mg/cm^2, 30kVp in "Investigation of the Imaging Characteristics of the $Y_2O_2S:Eu^{3+}$ phosphor for Application in X-ray Detectors of Digital Mammography". where, value difference in

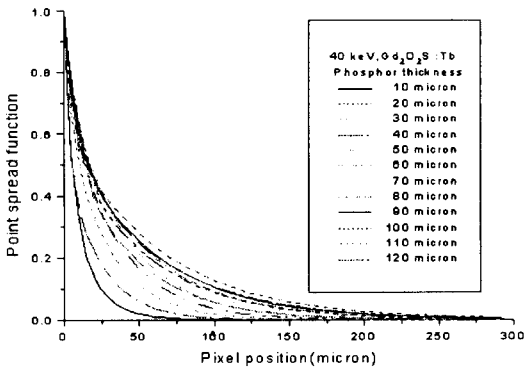

Fig. 9. PSF as Phosphor Thickness

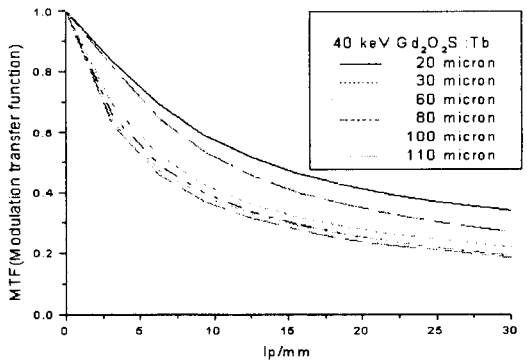

Fig. 10. MTF of Phosphor

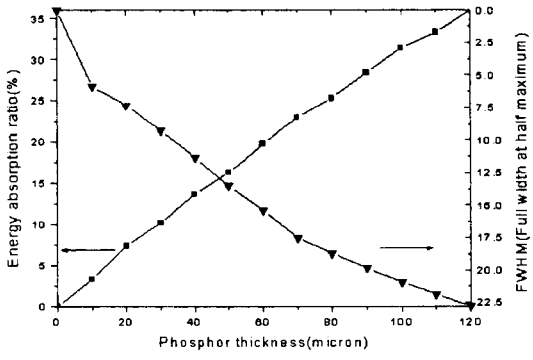

Fig. 11. Optimum Thickness Considered X-ray Absorption and Resolution

low resolution is defined by assume in this simulation.[1],[14]

3.2.4. Simulation Result

This simulation has done by 10~120 μm of Gd_2O_2S:Tb thickness and 40 keV of X-ray energy. So that X-ray absorption rate shows 3.3 %, 7.35 %, 10.15 %, 13.69 %, 16.3 %, 19.76 %, 22.95 %, 25.25 %, 28.37 %, 31.34 %, 33.27 %, 36 % every thickness each. Also, In this simulation, FWHM(Full Width at Half Maximum) of PSF as phosphor thickness shows 5.9 μm, 7.3 μm, 9.25 μm, 11.34 μm, 13.51 μm, 15.36 μm, 17.51 μm, 18.72 μm, 19.84 μm, 20.93 μm, 21.86 μm, 22.78 μm. Fig. 9 show PSF as Gd_2O_2S:Tb thickness and 40 keV of X-ray energy. Fig. 10 shows MTF, and optimum thickness show 48 μm such as Fig. 11 but it is changed by demand of resolution and X-ray absorption

4. Bonding of Fiber Optic Plate(FOP) and CCD

4.1. Characteristic of Fiber Optic

FOP is made a number of single fiber optic by thermal compress and used medium to transfer image. Generally, X-ray using phosphor use more than lense, because of high transmission efficiency. The principle of light photon in fiber optic is to transfer light signal by inner total reflection through core incident light photon which is caused the difference of core and refraction index of cladding surrounding core. Core is addition to high atom number material in SiO_2. Cladding is SiO_2.[11],[12] High atom number material is amount difference as manufacture company, also refraction index of core is 1.6~1.8 and cladding is 1.4~1.6.

In FOP of EEV Corp. core material is SiO_2 :LaReAgNb , density isrm 5.8 g/cm^3 and cladding is SiO_2B:La, density is 2.20 g/cm^3. FOP is reduced White noise occurring by direct X-ray not react with phosphor and expand CCD life. also, FOP prevent diffusion because it guide incident light.

Also, the important characteristic of fiber optic system is that it can collect a light that entered in large range angle as well. it represents with NA(Numerical Aperture). The equation defined NA can be used in every critical system including fiber optic. like Fig. 12, once θ is rotated, come into a critical circular cone. the incident ray out of the circular cone angle is attenuated not spread following fiber optic. because core and cladding have not same bending rate, occurs a reflection in the boundary surface. and if it is not enter into maximum critical angle, get out passed the core. Incident angel into the inside maximum critical angle of fiber optic is get out in the same angle

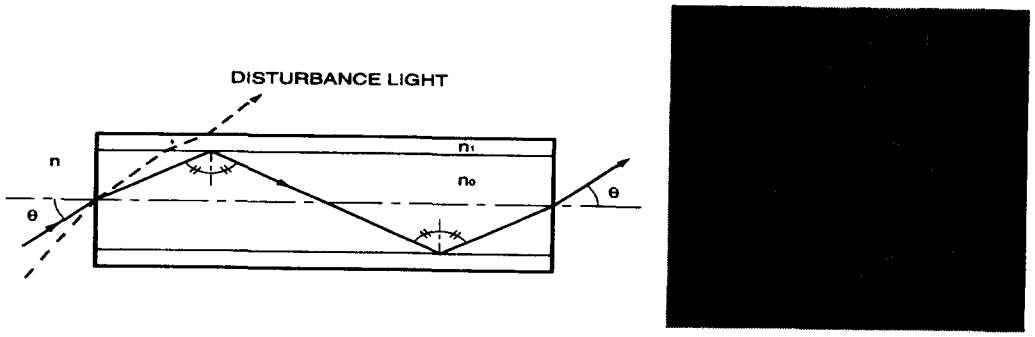

Fig. 12. Fiber Optic and Fiber Optic Plate

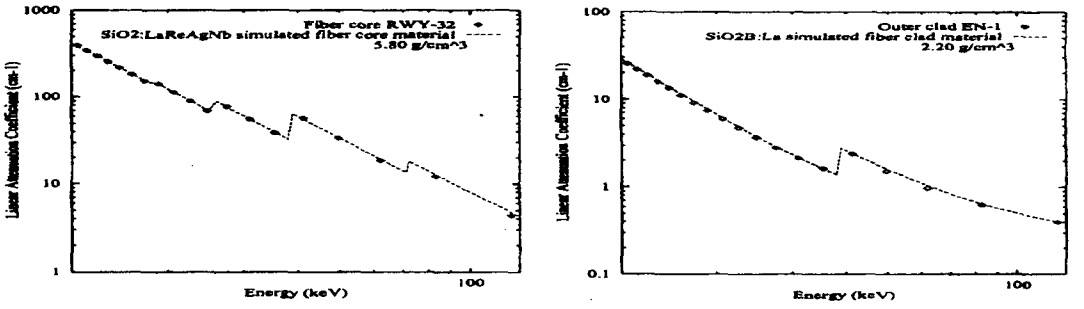

Fig. 13. X-ray Attenuation as Energy in Core and Cladding

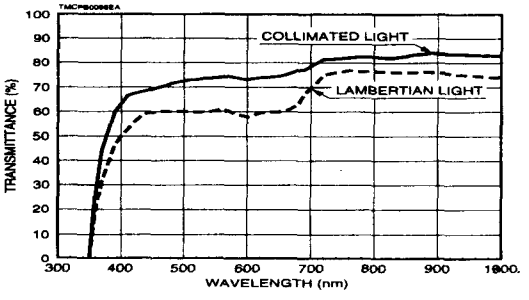

Fig. 14. Optic Transmission Rate of FOP as Optical Wave

when it get out of the fiber optic. Once the incident light inside critical angle has the different transfer rate every production company.

$$NA = n\sin\theta = \sqrt{n_0^2 - n_1^2} \quad (4)$$

Where, NA is Numerical Aperture, n is refraction index of air, n_0 is refraction index of core, n_1 is refraction index of cladding, θ is critical angle.

4.2. Effect of Image by FOP Bonding

FOP is combined with mono fiber optic which transfer light photon each fiber optic. Generally in union with CCD, due to miss pixel array it causes a very large resolution reduction by creating "Moire Stripes" gain image. In addition when it bend using optical adhesive, it can causes a resolution of gain image by air inflow at the bonding side. Fig. 15

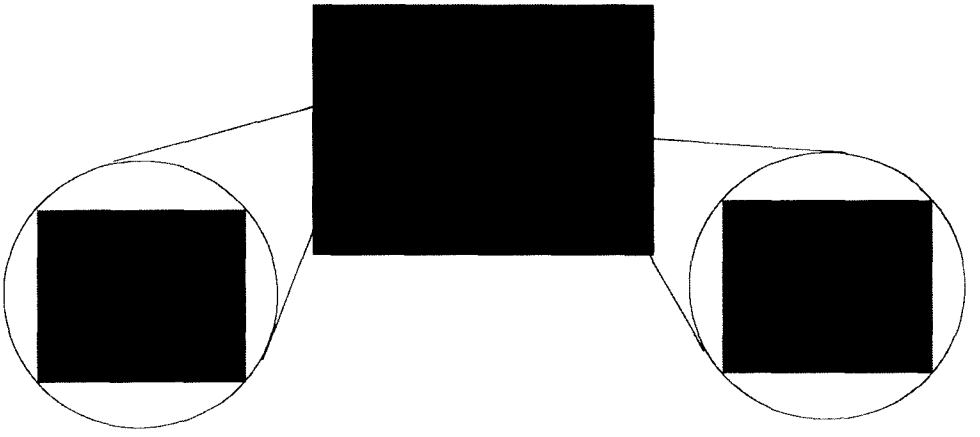

A) Air mottle B) Moire Stripes

Fig. 15. Resolution Damage by FOP Bonding

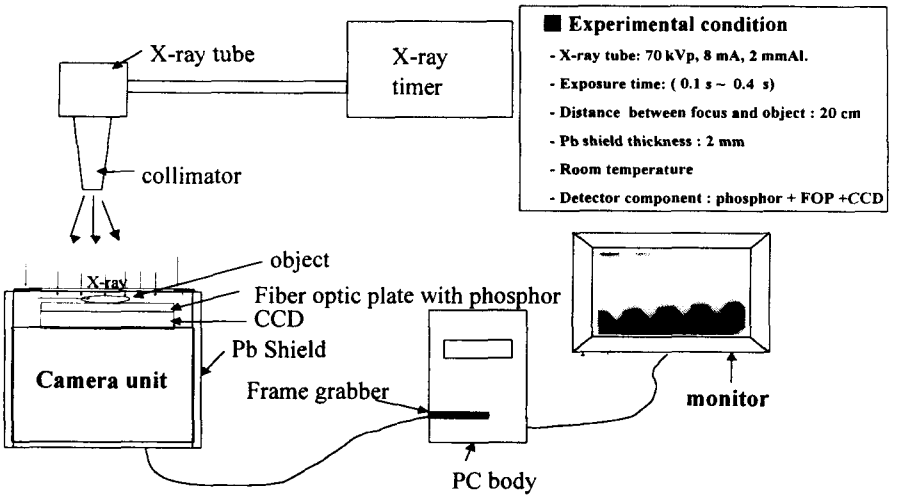

Fig. 16. Composition of Prototype X-ray Image System

shows Moire Stripes phenomenon occurred by disarray in the wave of 6 μm. FOP and 9.6 × 7.5 μm unit pixel, and air mottle occurred by an inflow of air as using of high viscosity optical adhesive optical adhesive we can developing this phenomenon using micro lense in CCD.

when FOP and CCD is bonded, some attention matters required.

① Viscosity of optical adhesive is to e below 100 cp if possible.

② The bending rate of FOP and adhesive is to be same or similar.

③ The thickness of optical adhesive keeps up with uniform and thinner than a half of CCD unit pixel if possible.

④ It is necessary that exact arary of unit optical fiber at FOP and unit pixel at CCD. if there is a little missed error, a very serious "Moire stripes" is occurred in the final result image.

⑤ Because CCD produced heat in operation, adhesion which considering the rate of heat expansion between silicon and FOP is demanded.

⑥ When adhesion, the bonding side of CCD and FOP must have cleared.

⑦ When adhesion, Don' t touch bonding wire around CCD valid pixel.

5. Prototype X-ray image system

5.1. Structure of X-ray Sensor and Characteristics

We composed a prototype X-ray image sensor like Fig.16 using FOP, Gd_2O_2S:Tb, 1/3 inch visible-ray black-white action image CCD camera, model of Samsung electronics, inc. Actually, to be used dental it' s sensor thickness is less than 6 mm because it enters intra-oral of a man.

In the characteristics of sensor, the camera is using interline transfer CCD, the way of a injection is 2:1 interlace. Photodiode fill factor of CCD is about 25 %, spectral sensitivity has a ideal state in 545 mm wave. About 50 %, number of pixel is 230,000. the size of unit pixel isrm 9.6 × 7.5 μm. Gd_2O_2S:Tb is a product of England Applied Scin.

Fig. 17. Image of Line Pair Phantom

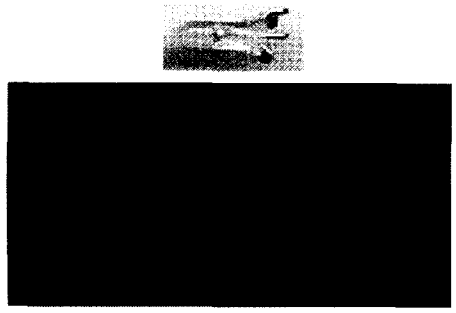

a) Light emit diode

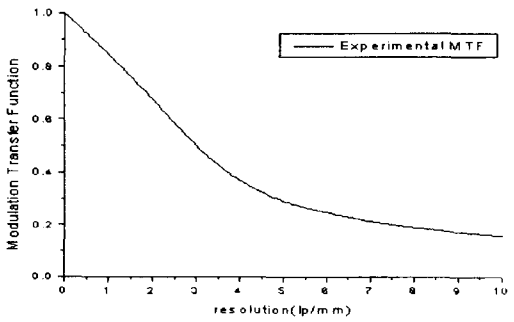

Fig. 18. MTF of Experiment Sensor

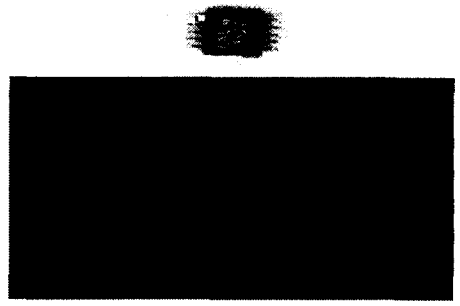

b) micro chip

Fig. 19. MTF of Experiment Sensor

micro powder has a 4 μm diameter, 25 mm/cm^2 thickness average. FOP is schott' s product, core and cladding rate is 7:3, thickness is 3 mm. The union of FOP and CCD was used optical adhesive agent No.366 form Loctite inc. To capture image real-time, we obtained an image using DT3152 frame grabber from Data Trans inc. X-ray generator is IRIX708, 70 kVp, 3 mA, 2 mmAl from Trophy inc. We use computer system Pentinum pro 200 MHz and capture S/W is programed by visual C.

5.2. Image Experiment and Result

Structured X-ray image sensor have a size of validity, 5×4 mm which is same that of tooth. we experimented image with this sensor. investment time of each experiment is 0.1~0.2 second. We checked that the limit resolution of this system is about 10 lp/mm which is in the MTF of gain image using resolution phantom image(Fig. 17) and edge method(Fig. 18).

Fig.19 is a image for photo-diode and micro chip, and irradiation time is 0.1, 0.2 second each. The black park above image is valid pixel part of space due to disarray as the result that using prototype system acquire a image, the limit resolution resulted in 10 lp/mm. we found that the causes of low resolution are quantum noise like white spot, structural bonding of phosphor and Moire stripes due to fiber optic plate disarray as well. As the limited resolution of dental digital X-

ray sensor which currently used differences in noise though we made a similar sensor. The low resolution caused by disarray can be solved by the structure of array equipment using considering condition referred before contrast can be developed by using micro lens of CCD pixel, applicable optimal phosphor thickness and image developing algorithm. The question about this must to be solved restructuring each element unite of sensor.

6. Results and Discussions

Phosphor thickness, FOP and CCD union were the most important criteria for obtaining good resolution image when creating indirect intra-oral X-ray image sensor. In the present study, phosphor displayed appropriate general CCD spectral sensitivity. On the other hand, Gd_2O_2S:Tb has been chosen for its good X-ray efficiency. Optimum thickness 48 μm considering X-ray absorption rate and PSF for 10~120 μm various thickness of Gd_2O_2S:Tb. The optimum thickness is different where is given more weight on X-ray efficiency or resolution. In this study, we gave equal weight on X-ray efficiency and resolution. We obtained a real time image having about 10 lp/mm resolution by realization of prototype X-ray image sensor like the structure of indirect intra-oral dental digital X-ray image sensor. Air bubbles and Moire stripes of bonding error at FOP causes a serious loss in resolution of obtain image. We found that the cause of this loss is to use the high density light adhesive and the disarray among pixels in the union of CCD and FOP. Also, we found that the important thing for prevention of resolution loss in FOP bonding is are to one array of unit optical fiber and CCD unit pixel. Except that, it is required that to improve the efficiency of light photon. The union thickness of FOP and CCD is less than 1/2 CCD pixels interval and we must use a low density light adhesive.

Next, optimum thickness calculated by simulation and improved obtain image composing alignment equipment of FOP and CCD require. By application 70 kVp continuous spectrum compression analysis with current result are also required.

8. References

1. Jacob Beutel, Harold L. Kundel, " Handbook of Medical Imaging, Volume 1. Physics and Psychophysics", SPIE PRESS, p229-253 (1998).
2. Priv. Doz. Dr, " Evaluation of the new RadioVisioGraphy system image quality", Oral Surg Oral Surg Med. Oral Pathol, Vol 72, p627-631, (1991).
3. Hamamatsu, "FOS for Digital X-ray imaging", Hamamatsu. Cat. No. TMCP9003E01, (1997).
4. Psul P. "CCDs Reduce Radiation Exposure at the Dentist' s",Laurin Publishing Co.,Inc, (1994).
5. Istvan Nadey, Stephen Ross,"Charge-coupled-devece/fiberoptic taper array X-ray detector for protein crystallographyl.", SPIE Vol.3019, (1997).
6. Andrew D A Maidment, Martin J Yaffe, "Analysis of signal propagation in optically coupled detectors for digital mammography: I. phosphor screens", phys. Mde. Biol. vol 40, p877, (1995)
7. Ho Kying Kim, Gyuseong Cho, "Monte Carlo studies of metal/phosphor screen in therapeutic X-ray imaging" Nucl. Instru. and Meth. in Phy. Res. A 422, p 71 3-717(1999).
8. Hans-Goran Grondahl, "An Image Plate System for Digital Intra-oral Radiography." Dental Radiography, (1996).

9. A Workman and DS Brettle, "Physical performance measures of radiographic imaging systems" Dentomaxillofacial Radiology, Vol 26, p 139-146, (1997).
10. SHANNON and WYANT, "Fiber Optics" Applied optics and optical engineering, Vol. 4, p1-29.
11. Glenn F.Knoll, "Radiation Detection and Measurement Third Edition", Wiley, (2000).
12. Michael J. Flynn, "Quantum Noise in Digital X-ray Image Detectors whith Optically Coupled Scintillators.", IEEE Trans.Nucl. Scie.,vol. 43, No.4 (1996).
13. G.F.Knoll, " Detector a Program for Modeling Optical Properies of Scintillator", TRIUMF, (1996).
14. Robert K. Swank, "Absorpiton and noise in x-ray phosphors.", General Electric Corporate Research and Development, (1973).